

Synthesis and characterization of crystalline powder NiO and NiMn₂O₄ obtained by sorbitol-based route

Cabral, A. J. F.; Costa, L. S.; Ferreira, V. S.; Remédios, C. M. R.

Federal University of Pará, Belém, Pará, Brazil
*remedios@ufpa.br

[Clique aqui para digitar texto.](#)

Abstract—Crystalline powders of nickel oxide (NiO) and nickel manganite (NiMn₂O₄) were synthesized by new and simple chemical route which is based on the use of sorbitol as a chelating agent under low temperatures, ambient pressure and neutral pH. The samples obtained were analyzed by X-ray powder diffraction and scanning electron microscopy as a function of firing temperature, heating rate and firing time. The average crystallite size (D) was estimated by Scherrer's equation. Results analysis confirm one single phase of cubic NiO at 500 °C and cubic spinel NiMn₂O₄ at 800 °C.

sol-gel; X-ray; nickel oxide; nickelmanganite;

I. INTRODUCTION

The interest in 3d-series metal oxides has increased in the last decades because of the different physical and chemical properties encountered in the nanocrystal, thin film and their corresponding bulk. Among the transition metal oxides, nickel oxide (II) received a lot of attention due to its various applications in several technological fields. It can be used in catalysis [1], gas sensors [2, 3], fuel cell electrodes [4], conversion of solar cells, green pigments, thermal protection and others [5, 6]. Nickel oxide (II) is a p-type semiconductor because it has structural defects that can be caused by vacancy of Ni ions [7]. Moreover, it is known as an antiferromagnetic material below 523 K [8].

Another important oxide is the nickel manganite, which is a ferrimagnet [9] and its main application is as a negative temperature coefficient (NTC) thermistor [10]. It crystallizes in a partially inverse cubic spinel structure where nickel and manganese ions are distributed among the tetrahedral and octahedral sites [11]. Controlled synthesis of nickel manganite (including size and morphology) has attracted significant interest.

Several methods have been proposed to the synthesis of NiO and NiMn₂O₄ in the polycrystalline form. The chemical route using commercial gelatin as an organic precursor stands out because to be simple relatively and inexpensive. Unfortunately, the material produced may be contaminated with various metals present in the composition of commercial gelatin [12, 13].

Our goal is to synthesize single phases of nickel oxide and nickel manganite by simple route of an aqueous sol-gel process based on the use of sorbitol as a chelating agent. The samples obtained were analyzed by X-ray powder diffraction (XRPD) and scanning electron microscopy (SEM). We will also analyze the morphology and size particles taking into account the synthesis parameters as heating rate and firing time.

II. MATERIALS AND METHODS

The reagents used to obtain the oxides were hexahydrated nickel chloride (NiCl₂·6H₂O, 99.9%, VETEC), tetrahydrate manganese chloride (MnCl₂·4H₂O, 99%) and sorbitol 70% (C₆H₁₄O₆). These materials were used without any further purification. In this process, the sorbitol is used as chelating agent to capture Ni and Mn ions in homogeneous solution and may also provide oxygen for the oxide formation. The NiO and NiMn₂O₄ powder samples were synthesized according to the following steps: 1) To synthesize NiO was prepared a homogeneous solution by dissolving 5.114 g of nickel chloride in 20 ml of distilled water at 50 °C and constant agitation, whereas for the synthesis of NiMn₂O₄ were prepared two homogeneous solutions: (i) one by dissolving 4.756 g of nickel chloride in 20 ml of distilled water at 50 °C (ii) other by dissolving 7.933 g of manganese chloride in 20 ml of distilled water at 50 °C; 2) To synthesize NiO was added 1.5 ml of sorbitol and to synthesize of NiMn₂O₄ was added 6 ml of sorbitol gradually to a beaker containing the metallic salt solution; 3) the polyalcohol and metal salt aqueous solution was stirred for 15 min at 50 °C to complete homogenization; 4) the viscous solution was placed in oven at 70 °C for 48 h

(the purpose of this step is the elimination of the solvent to form the gel); and 5) finally the gel was thermally treated at temperatures between 400 and 900 °C in air atmosphere.

The X-ray powder diffraction (XRPD) measurements were performed using a PANalytical X'Pert Powder diffractometer equipped with a CuK α radiation tube. The crystalline phases were identified using the diffraction database from the International Center for Diffraction Data (ICDD). Rietveld refinement analysis [14] was performed for all diffraction patterns using the DBWS 9807-Tools code [15]. The pseudo-Voigt function has been used to fit the peak profiles of the identified crystalline phases. The average crystallite sizes were estimated by Scherrer formula [16]. Scanning electron microscopy was carried out on a JEOL JSM-6490 LV scanning electron microscope with an accelerating voltage of 30 KV.

III. RESULTS AND DISCUSSION

Figure 1 shows the fit of the intensity calculated (red line) using the Rietveld refinement method applied to the experimental XRPD patterns (empty black dots) and as well as the difference between observed and calculated profiles. The XRPD pattern for sample calcined at 300 °C is a characteristic diffraction pattern of the amorphous material. The XRPD pattern of the sample synthesized at 400 °C is of face-centered cubic (fcc) crystalline phase of NiO. Impurity peaks were not observed, but a careful analysis in the background reveals the presence of amorphous material, probably part of the organic precursor remained.

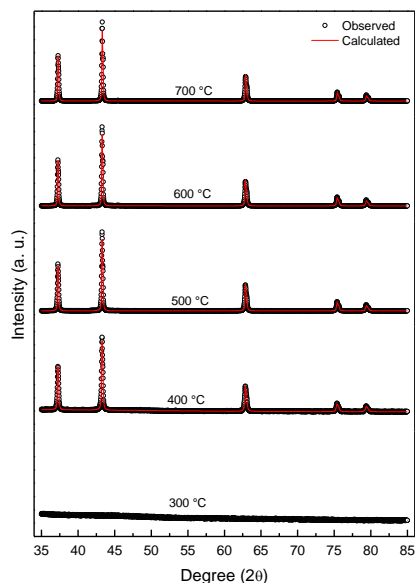


Figure 1. Calculated and experimental XRD patterns of the NiO sample calcined at 300, 400, 500, 600 and 700 °C.

In Fig. 1, the positions of the diffraction peaks and their relative intensities indicate that the samples produced at 500, 600 and 700 °C are also of the fcc NiO phase without any

other phase. It is noted that crystallite size increases with temperature. The lattice parameters of NiO sample calcined at 400 °C, 500 °C, 600 °C and 700 °C are 4.1796 (1) Å, 4.1780(1) Å, 4.1775 (2) Å and 4.1777 (1) Å respectively. The lattice parameter expands with the decreasing crystallite size. This effect may be caused by vacancy Ni ion. A similar behavior has also been observed previously for NiO nanoparticles [17, 18].

SEM images reveal the particle morphology and size of the sample synthesized at 400 °C. In Fig. 2a, we can see amorphous material mixed crystalline particles that have typical sizes in the range of 250 - 500 nm. We can see in Fig. 2b that sample synthesized at 500 °C has well defined octahedral morphology, which is free of amorphous material and has a typical particle about 500 nm.

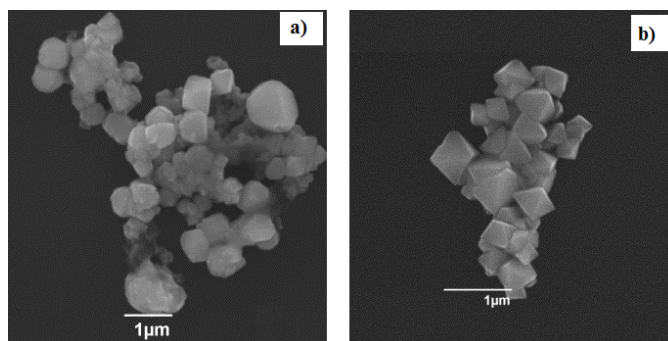


Figure 2. SEM images of NiO synthesized at a) 400 °C and b) 500 °C.

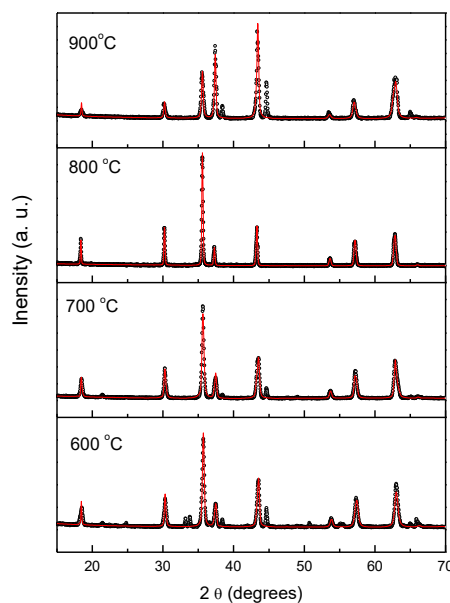


Figure 3. Experimental and calculated XRD patterns of the NiMn₂O₄ sample calcined at 600, 700, 800 and 900 °C.

Figure 3 displays the experimental XRPD patterns of samples prepared at temperatures between 600 and 900 °C for 4 h using heating rates of 10 °C/min, as well as the correspondents simulated patterns by Rietveld refinement. Samples fired at 600, 700 and 900 °C show additional diffraction peaks that can be associated with the reflections from several phases such as Ni_6MnO_4 , NiMnO_3 , MnO_2 and MnO_3 . However, samples fired at 800 °C do not show additional diffraction peaks, only the peaks of the cubic spinel NiMn_2O_4 phase are observed. According to this result, the best firing temperature for the production of pure NiMn_2O_4 is 800 °C.

For investigate the effect of firing times on the crystallite size a number of samples were prepared at 800 °C with firing times varying between 6 and 8 h using heating rates of 10 °C/min (Fig. 4).

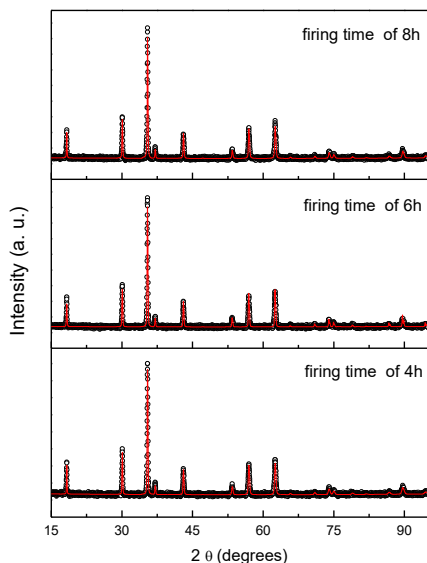


Figure 4. Experimental and calculated XRD patterns of the sample calcined at 800 °C with firing times varying between 6 and 8 h.

The lattice parameters are very similar in all samples, with values around 8.396 (1) Å.

To investigate the effect of the heating rate, we carried out X-ray powder diffraction and scanning electron microscopy experiments which demonstrated that a lower heating rate favors to sample purity. The SEM micrograph of the nickel manganite obtained at 800 °C shows the formation of agglomerates comprising particles with octahedral shape. Different heating rate produced very different particle sizes. Figure 5 shows two representative SEM images. The particle sizes of the NiMn_2O_4 were found to be between 150 nm and 600 nm with heating rate of 20 °C/min (Fig. 9a) and between 0.5 μm and 1 μm, with heating rate of 10 °C/min.

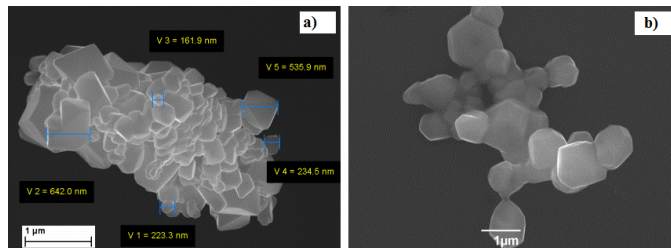


Figure 5. SEM images of NiMn_2O_4 synthesized at 800 °C a) with heating rate of 20 °C/min and b) with heating rate of 10 °C/min.

So, from scanning electron microscopy experiments, we conclude that the average particle size decreases with increasing heating rate. Unfortunately, from X-ray diffraction results, sample purity also decreases with increasing heating rate. We conclude too that the best heating rate for the production of pure NiMn_2O_4 is 10 °C/min.

IV. CONCLUSION

In this work NiO and NiMn_2O_4 crystalline powders were synthesized by a novel and simple aqueous sol-gel method based on the use of sorbitol as a chelating agent. The results of DRX indicated that the product of the process was successfully synthesized, i.e. without any spurious phase. The 800 °C is the best firing temperature for the production of pure NiMn_2O_4 . With the increasing of firing times the average crystallite size of NiMn_2O_4 increases whereas the average particle size decreases with increasing heating rate.

REFERENCES

- [1] S. Berchmans, H. Gomathi, G. Prabhakara Rao, J. Electroanal. Chem. 394 (1995) 267.
- [2] J. Barker, R. Pynenburg, R. Koksang, M.Y. Saidi, Electrochim. Acta, 41(1996) 2481.
- [3] R.C. Makkus, K. Hemmes, J.H.W. de Wit, J. Electrochem. Soc. 141 (1994) 3429.
- [4] H.R. kunz, J. W. Pandolfo, J. Electrochem. Soc. 139 (1992) 1549.
- [5] O. Palchik, S. Avivi, D. Pinkert, A. Gedanken, Nanostruct. Mater. 11 (1999) 415.
- [6] Y. Hamakawa, H. Hoshiya, T. Kawabe, Y. Suzuki, R. Arai, K. Nakamoto, M. Fuyama, Y. Sugita, IEEE Trans. Magn. 32 (1996) 149.
- [7] H. Sato, T. Minami, S. Takata, T. Yamada, Thin Solid Films. 236 (1993) 27.
- [8] L.C. Bartel, B. Morosin, Phys. Rev. B. 3 (1971) 1039.
- [9] S. Asbrink, A. Waikowskat, M. Drozdt, E. Taliks, J. Phys. Chem. Solids. 158 (1997) 725.
- [10] G.D.C. Csete de Györgyfalva, I.M. Reaney, J. Eur. Ceram. Soc. 21 (2001) 2145
- [11] A.P.B. Sinha, N.R. Sanjana, A.B. Biswas, Acta Cryst. 10 (1957) 439.
- [12] J.M.A. Alameida, C.T. Meneses, A.S. de Menezes, R.F. Jardim, J.M. Sasaki. J. Mag. Mag. Mater. 320 (2008) e304.
- [13] C.M.R. Remédios, J.M. Sasaki, Powder Diffr. 23 (2008) s56.
- [14] H.M. Rietveld, Acta Crystallogr. 22 (1967) 151.
- [15] L. Bleicher, J.M. Sasaki, C.O. Paiva-Santos, J. Appl. Cryst. 33 (2000) 1189.
- [16] L.V. Azároff, M.J. Buerguer, The Powder Method in X-Ray Crystallography, McGraw-Hill, 1958.
- [17] L. Li, L. Chen, R. Qihe, G. Li, Appl. Phys. Lett. S89 (2006) 134102.
- [18] W.J. Duan, S.H. Lu, Z.L. Wu, Y.S. Wang, J. Phys. Chem. C. 116 (2012)